Kinetic isolation of persistent radicals and application to polymer–polymer reactions

Erdem Karatekin
Department of Chemistry, Columbia University, New York, New York 10027

Ben O'Shaughnessy[a]
*Department of Chemical Engineering and Applied Chemistry, Columbia University, New York,
New York 10027*

Nicholas J. Turro
Department of Chemistry, Columbia University, New York, New York 10027

We analyze the transient kinetics of a mixture of two radicals (M and P), one of which (P) has very low, or zero self-reactivity (i.e., P is a ''persistent'' radical). For the case where the self-reactivity of the persistent radical is zero, we find a critical value for the initial concentration ratio $r \equiv P_0/M_0$, above which the persistent radicals are isolated at long reaction times after all of the M's react. If r is below its critical value the surviving fraction of P is zero. An experiment employing virtually zero self-reactivity nitroxide radicals is proposed to test the predicted critical behavior. If the self-reactivity of the M is stronger than the cross-coupling reactivity, then the critical value of the ratio r is negative, and a finite fraction of the persistent P radicals are always isolated, regardless of the initial concentration ratio r. For the case where the self-reactivity of the persistent radicals is finite but small, we find similar behavior, except now the P radicals react with one another on a much longer time scale following their isolation. The isolation process facilitates the measurement of $P–P$ reaction kinetics in situations where it is difficult to generate the P radicals by themselves. An experiment to measure fundamental polymer–polymer reaction kinetics in concentrated solutions or melts is proposed based on these ideas. © *1998 American Institute of Physics.* [S0021-9606(98)50422-9]

I. INTRODUCTION

Reactions involving free radical intermediates are encountered frequently in chemistry and in biology.[1–3] The kinetics of such reactions is interesting for many reasons. For example, such radical–radical reactions are excellent testing grounds for fundamental theories on diffusion-controlled reactions.[4–8] This is due to the very high local reactivities of radicals: only a few encounters between the radical groups are needed for reaction to take place.

In this article we study the transient kinetics of a mixture of radicals in the peculiar case when one type of the radical species present in the mixture has very low, or zero ''self-reactivity''.[2,9] That is, the bimolecular reactions of these radicals with their own kind occur with a rate constant that is very small.[10] The presence of radicals with low self-reactivity in radical–radical reactions gives rise to quite interesting kinetic phenomenology. Of particular interest to us is to establish whether and under what conditions only the species with low self-reactivity survive at long reaction times from a mixture initially containing other radicals as well. Once the species with low self-reactivity has been isolated, their bimolecular reactions with their own kind can be studied without interference from the other radicals which were

present earlier. An application of this concept to the study of macroradical–macroradical reactions was our original motivation. Specifically, we were interested in the isolation of macroradicals from a mixture initially containing small molecule radicals and polymer radicals in order to study macroradical–macroradical reaction kinetics. The degree of polymerization and concentration dependence of the reaction rate constant for such polymer–polymer reactions is of fundamental interest.[11–13] The traditional method of measuring such rate constants, phosphorescence quenching,[11,14,15] fails at high polymer concentrations and/or degrees of polymerizations, due to the limited range of phosphorescence lifetimes: excitation decays via first order processes before a chain carrying a phosphorescent label can encounter another chain which is labeled with a quencher. By contrast, the pseudo-first-order decay of macroradicals can be made to take place at much longer time scales than those accessible by phosphorescence, by the appropriate choice of conditions.[16] That is, such pseudo-first-order decays can be made negligible in macroradicals compared to second order bimolecular processes, even in a polymer melt where it may take seconds for a polymer coil to move over a distance comparable to its radius of gyration.[17,18]

There are many other situations where a species with low self-reactivity is present in a mixture with other (highly self- and cross reactive) radicals. For example, in a mixture

---
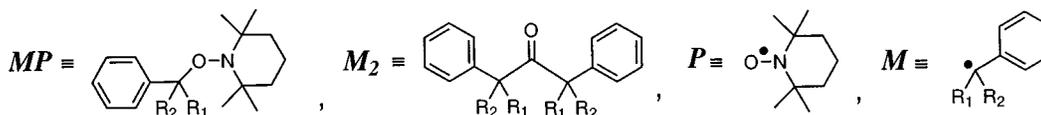[a]Author to whom correspondence should be addressed.

of radicals confined in a zeolite framework, the movement of some of the radicals that are present may be slowed down more severely than the others due to their sizes/shapes.[19] Both macroradical–macroradical reactions and the reactions of radicals confined in zeolite networks are of enormous industrial importance. In both of these examples the high self-reactivity of an ordinary radical is suppressed due to the slowing down of its movement, either because it is attached to a slowly moving long chain polymer, or because it is confined in a crystal network.

On the other hand, there are many cases where the low self-reactivity of a radical species is due to its local chemical structure. Perhaps the best known types of such radicals are the nitroxide type radicals[20] (see the radical P in Scheme I) which appear in living free radical polymerization,[21–25] spin trapping reactions,[20] polymer stabilization (e.g., by hindered amine light stabilizers—HALS[26,27]), radical scavenging reactions, etc. Some other radical types displaying similarly low self-reactivity are quinone type radicals which arise in the inhibition of free radical chain reactions by phenolic compounds,[28] some cobalt compounds,[29,30] and nitric oxide radicals[31] which have important biological roles.

Consider a mixture of two radicals, M and P, created at a certain time by a laser pulse. We follow the decay of these radicals from their initial concentrations, $M(0) \equiv M_0$, $P(0) \equiv P_0$, in the case where one of the species (say P) has very low reactivity with radicals of the same type, but is still being very reactive with the other type, M. That is, the reactions we consider are,

$$M + M \xrightarrow{\frac{1}{2} k_{MM}} M_2, \quad M + P \xrightarrow{k_{MP}} MP, \quad P + P \xrightarrow{\frac{1}{2} k_{PP}} P_2, \tag{1}$$
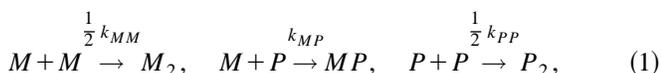
with the rate constant for the P–P reactions being much less than the other rate constants, that is $k_{PP} \ll k_{MP}$, and $k_{PP} \ll k_{MM}$.

The concentrations of the radical species will obey

$$\dot{M} = -k_{MP}MP - k_{MM}M^2,$$
$$\dot{P} = -k_{MP}MP - k_{PP}P^2. \tag{2}$$

Note that the steady state kinetics of the system just described has been studied theoretically by Hanns Fischer,[9] and the predictions of the theory were later tested by experiment.[28] The present study, on the other hand, addresses the question of *transient* kinetics.

We first consider, in Sec. II, the simplest case where the rate constant k_{PP} is equal to zero. We then try and answer the question: does one end up with only the P species as time tends to infinity, and if so what is the surviving fraction of the P species? Most surprisingly, we show that under certain conditions one is left with only the P species as time $\to \infty$, *regardless of the initial concentration of P!*

In many practical situations, however, the self-reactivity of the P will be finite. This is very similar to the zero self-reactivity case, except now after a certain time the great majority of the species present in the mixture will be the P species under certain conditions. That is, the species with the low self-reactivity will be kinetically isolated. This is dealt with in Sec. III. In Sec. IV, we show how the analyses of the previous sections can be applied in a particular experiment designed to isolate monodisperse polymeric radicals to measure macroradical–macroradical reaction rate constants.

II. COMPLETE ABSENCE OF SELF-REACTIVITY IN ONE SPECIES: $k_{PP} = 0$

The self-reactivity of some types of radicals, such as nitroxides, is so low[10] that it can be considered to be zero on experimental time scales, that is $k_{PP} = 0$. For example, consider the model system shown below in Scheme I.

$$MP \equiv \quad , \quad M_2 \equiv \quad , \quad P \equiv \quad , \quad M \equiv$$

Scheme I.

A mixture containing an arbitrary composition of the species MP, M_2, and P of this system is flash photolyzed to create M and fresh P species, as shown in Fig. 1.

We will see below that two key parameters which determine the kinetics of this reaction system are the initial ratio of reactant concentrations, r, and a dimensionless measure, ω, of the difference between the rate constants,

$$r \equiv \frac{P_0}{M_0}, \quad \omega \equiv \frac{k_{MP} - k_{MM}}{k_{MP}}. \tag{3}$$

Note that in experiments of the type described above, the parameter r can be tuned from zero to infinity, by starting from a mixture of MP, M_2, and P of any desired composition and then using a laser flash to generate the initial mixture of M's and P's. Reactions can then be monitored by suitable spectroscopic techniques, such as electron paramagnetic resonance[32] (EPR), ultraviolet-(UV-VIS) absorption,[16] etc. The prospect of tuning r is particularly interesting, since, as will be seen shortly, a critical point exists at $r = r_c^0 \equiv \omega$ separating two distinct classes of kinetic behavior. The parameter ω depends on the local chemical properties of the radicals and varying it would require changing the radical structures.
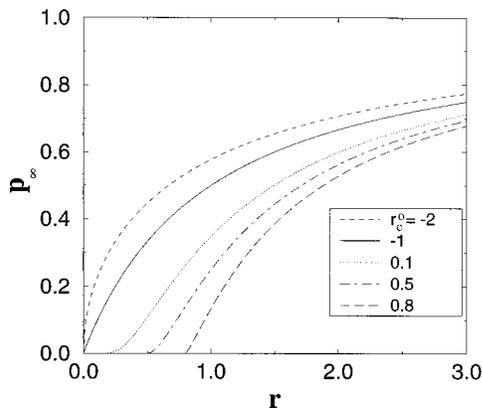
FIG. 1. A mixture of the precursor M_2 and the zero self-reactivity P radicals is photolyzed by a laser flash to create highly self and cross-reactive M radical pairs, a finite fraction of which escapes. M–P cross-coupling reactions and M–M self coupling reactions are thus switched on. The initial density of the radicals can easily be adjusted (by adjusting the amount of M_2 and P prior to the laser flash, or by adjusting the laser intensity) so that experimentally the parameter $r \equiv P_0/M_0$ can be tuned through its critical value, $r_c^0 \equiv 1 - k_{MM}/k_{MP}$. During the subsequent kinetics, for $r \lesssim r_c^0$, persistent P radicals disappear as $t \rightarrow \infty$, while for $r > r_c^0$ a finite fraction is left over after all M radicals have reacted.

Let us first establish the trajectory in the M–P plane followed by the reaction mixture as time progresses. In fact it is more convenient to follow trajectories in the m–p plane where m and p are concentrations scaled by their initial values

$$m \equiv \frac{M}{M_0}, \quad p \equiv \frac{P}{P_0}. \tag{4}$$

Eliminating the time variable in Eq. (2), one has

$$\frac{\dot{m}}{\dot{p}} = \frac{dm}{dp} = (1-\omega)\frac{m}{p} + r, \tag{5}$$

which can readily be solved after defining an auxiliary variable $y \equiv m/p$. The solution is

$$m = \frac{r}{r_c^0}p + \left(\frac{r_c^0 - r}{r_c^0}\right)p^{1-r_c^0}, \quad r_c^0 \equiv \omega \neq 0. \tag{6}$$

From Eq. (6) we see that there are two classes of trajectories, depicted in Fig. 2, depending on the magnitude of the initial ratio of concentrations of low self-reactivity P to the fast reacting M species. If and only if this ratio is sufficiently large, a finite concentration of P radicals, $p_\infty P_0$, is always left behind after all reactions are complete,

$$p(t=\infty) \equiv p_\infty = \begin{cases} [1 - r_c^0/r]^{1/r_c^0} & (r > r_c^0) \\ 0 & (r < r_c^0) \end{cases}, \quad r_c^0 \equiv \omega. \tag{7}$$

Now, for a given set of reacting species, r_c^0 is a fixed parameter, in most cases of order unity. The interesting variable for the experimentalist is r, which can be varied with ease. From Eq. (7), one sees that if it happens that the cross-coupling reactivity is weaker than the M self-reactivity, i.e., $k_{MM} > k_{MP}$, then r_c^0 is negative and a finite fraction of P will *always* survive, regardless of the initial concentration ratio r. This is perhaps the most interesting conclusion in this article.

When the reverse inequality holds, $k_{MM} < k_{MP}$, then r_c^0 is positive and a finite number of P will only survive provided $r > r_c^0$. Tuning the concentration ratio r, one can then pass through the critical value $r = r_c^0$ separating trajectories with positive and negative curvature (see Fig. 3). This special trajectory is the straight line $m = p$ (see Fig. 2).

FIG. 2. Characteristic trajectories followed by scaled concentration variables $m \equiv M/M_0$ and $p \equiv P/P_0$ in the m–p plane are depicted. Trajectories commence at $(p,m) = (1,1)$ and follow curves as indicated by arrows as time progresses. Two very different classes of trajectories are predicted, depending on initial concentration ratio, $r \equiv P_0/M_0$: (i) for $r < r_c^0 \equiv \omega \equiv 1 - k_{MM}/k_{MP}$ all of the P species are consumed as the M's disappear, whilst (ii) for $r > r_c^0$ a finite fraction p_∞ [Eq. (7)] of the persistent P radicals survives after all M's have reacted. The two classes of trajectories are separated by the critical line $m = p$, which is realized when $r = r_c^0$. For trajectories above the critical line ($r < r_c^0$) the curvature is always positive and the final approach to the origin is with infinite slope. Trajectories below the critical line have negative curvature, and have finite slope as p_∞ is approached.

In Fig. 4 we have graphed the dependence of p_∞ on r (at several fixed values of r_c^0). An interesting feature is the location of the inflection point at $r = (\omega + 1)/2$ whose measurement provides a rather interesting experimental method of determining the ratio of rate constants k_{MM}/k_{MP}.

In Fig. 2 we have indicated various other prominent features which we believe are experimentally accessible: The initial trajectory slope is $1 + r - \omega$, and the final slope is either equal to r (when $r > r_c^0$) or is infinite (when $r < r_c^0$).

To end this section let us briefly consider the kinetics. In all of the cases considered above there is a single characteristic time scale, $\tau \equiv 1/(k_{MP}P_0)$, for the decay of the P spe-

FIG. 3. By changing the concentrations of the M_2 and/or P species shown in Scheme I and in Fig. 1, or by varying the laser intensity, one can tune the initial concentration radical concentration ratio, $r \equiv P_0/M_0$, such that it passes through its critical value, $r_c^0 \equiv \omega \equiv 1 - k_{MM}/k_{MP}$. As r is decreased from a value greater than unity, the asymptotically surviving fraction of persistent P radicals, p_∞ of Eq. (7), decreases and reaches zero as $r \rightarrow r_c^0$.

FIG. 4. The surviving fraction, p_∞, of the persistent P radicals is plotted for various (fixed) values of the critical initial concentration ratio, r_c^0, as a function of initial concentration ratio, r. The surviving fraction p_∞ is finite for $r>r_c^0$ and zero for $r<r_c^0$. When the cross-coupling reactivity is weaker than the M self-reactivity, $k_{MP}<k_{MM}$, r_c^0 is negative and p_∞ is finite for *any* $r>0$. The inflection point occurs at $r=(r_c^0+1)/2$ (for $-1<r_c^0<1$), whose measurement provides a rather interesting and accurate method of determining the ratio of the rate constants k_{MM}/k_{MP}.

cies. The final approach ($t\gg\tau$) of p to its asymptotic value p_∞ occurs either as an exponential decay (when $r>r_c^0$ and p_∞ is finite) or as a power law (when $r<r_c^0$ and p_∞ is zero),

$$p-p_\infty\approx\begin{cases}\exp\{-p_\infty t/\tau\} & (r>r_c^0)\\ \text{const.}(\tau/t)^{1/(1-\omega)} & (r<r_c^0)\end{cases},\quad r_c^0\equiv\omega. \quad (8)$$

The comments above apply assuming r and w are away from their special values, $r=r_c^0$ and $\omega=1$.

III. LOW SELF-REACTIVITY IN ONE SPECIES: $k_{PP}\ll k_{MP}$

The previous section examined the ideal case where the self-reactivity of the persistent P radical vanished. In real situations this will of course be finite and may have important experimental consequences. Let us now generalize the previous analysis to the case where k_{PP} is finite but still much smaller than both k_{MP} and k_{MM}. That is, the quantity ϵ is now finite but small,

$$\epsilon\equiv\frac{k_{PP}}{k_{MP}}\ll 1. \quad (9)$$

We will find very similar behavior to that of the previous section in that for sufficiently large initial P concentration the nonpersistent M species virtually disappears, leaving behind a finite concentration of P radicals. There is a fundamental difference, of course: these P radicals eventually react with one another and disappear, on a much longer time scale. That is, the early episode results in isolation of the P radicals, facilitating observation of $P-P$ reaction kinetics thereafter. An application of this concept to the study of polymer–polymer reaction kinetics in concentrated solutions or melts will be discussed in the next section.

As in Sec. II, we first establish the trajectories in the plane of the scaled concentrations, m and p. Eliminating the time variable in Eqs. (2), one has
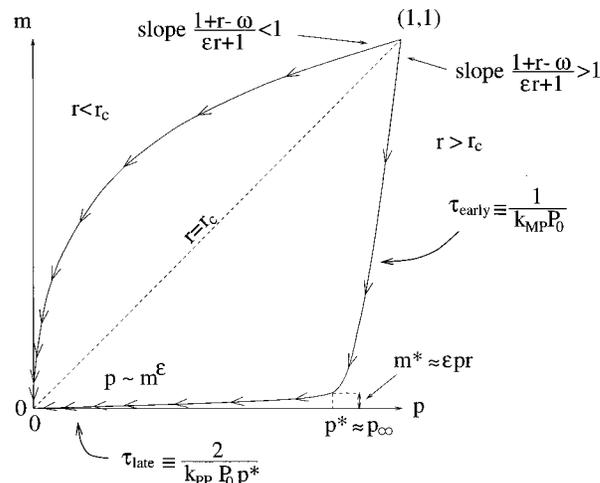
FIG. 5. For finite but small P self-reactivity, $\epsilon\equiv k_{PP}/k_{MP}\gg 1$, the behavior is very similar to the case $\epsilon=0$ (Fig. 2) in that for sufficiently high initial P concentration $[r>r_c\equiv\omega/(1-\epsilon)]$ a fraction $p^*\approx p_\infty$ of the persistent P radicals is essentially isolated from the initial mixture. This isolation process occurs on a time scale $\tau_{\text{early}}\equiv 1/(k_{MP}P_0)$ during which the cross coupling and M self reactions are dominant. The fundamental difference relative to $\epsilon=0$ is that these surviving P species react with one another following their isolation and disappear on a much longer time scale, $\tau_{\text{late}}\equiv 2/(k_{PP}P_0 p^*)$. During this late period, reactions are primarily of $P-P$ type. Hence, by isolating P radicals and measuring τ_{late} one can obtain k_{PP} directly. This may be useful in cases where it is difficult, or impossible, to generate the P species by themselves. An application of this concept to the study of polymer–polymer reaction kinetics is discussed in the text.

$$\frac{dm}{dp}=\frac{(1-\omega)(m/p)^2+r(m/p)}{\epsilon r+(m/p)}. \quad (10)$$

As for $k_{PP}=0$ [cf. Eq. (6)], there exist two classes of trajectory, depending on the initial concentration ratio r, as depicted in Fig. 5. Along the critical line separating these two classes one has $dm/dp=m/p=1$, whence $r=r_c\equiv\omega/(1-\epsilon)$, after using Eq. (10) (cf. $r_c=\omega$ for $k_{PP}=0$).

The trajectories which lie above the critical line in Fig. 5, $r<r_c$, are essentially the same as those obtained in Sec. II for $r<\omega$ (cf. Fig. 2) to within small errors. It is shown in Appendix A that for these trajectories m/p always increases as p decreases and that the curvature is always negative. It follows that $m/p\gg\epsilon r$ is true for the entire trajectory, and Eq. (10) to leading order is unchanged from Eq. (5) for the $\epsilon=0$ case. Physically this makes sense: the fact that P species can react with one another is unimportant, since the concentration of P never reaches a value much greater than that of M. Consider now $r>r_c$ trajectories, lying below the critical line. For these the curvature in the $m-p$ plane is always positive (see Appendix A). Each trajectory now exhibits two distinct regimes (see Fig. 5). Let us start from $(1,1)$, and describe the trajectory as p decreases to zero. Now during the "early" stages one has $m/p\gg\epsilon r$; thus the ϵr term in Eq. (10) is irrelevant and the trajectory is essentially the same as for $k_{PP}=0$. However, since m/p is always decreasing as p decreases (see Appendix A), there comes a point where this term changes the behavior; this happens when $m/p\approx\epsilon r$, which implies $p\approx p_\infty$ using Eq. (6) with m set to zero (correct to leading order). Here p_∞ is the asymptotic value for

$k_{PP}=0$, $r>r_c$, Eq. (7). Thus a second ("late") phase of the trajectory commences at (m^*,p^*) where

$$m^* \approx \epsilon r p_\infty, \quad p^* \approx p_\infty. \tag{11}$$

Note that these values correspond to the moment when the $P-P$ reaction rate first becomes comparable to the $M-P$ reaction rate, $k_{PP}P^2 \approx k_{MP}MP$. From this point onward, $P-P$ reactions are dominant and m/p continues to decrease; solving Eq. (10) with $m/p \ll \epsilon r$ one finds a simple power $p \approx m^\epsilon$. During this phase m is essentially zero, and p decays in time as if there were only P species in the system (see below).

In summary, the trajectories for $r<r_c$ are approximately given by Eq. (6) whilst for $r>r_c$ one has

$$m \approx \begin{cases} (r/\omega)p+[(\omega-r)/\omega]p^{1-\omega} & (p \gtrsim p^*) \\ p^{1/c} & (p \ll p^*) \end{cases}, \quad (r>r_c). \tag{12}$$

We remark that these relations hold only provided ω and r are not too close to their special values, $r=r_c$ and $\omega=1$.

We close this section with a few simple comments on the kinetics. When $r<r_c$, kinetics are virtually unchanged from those described in Sec. II. This is also true for the $r>r_c$ family during the "early" regime only, $p \gtrsim p^*$, when there is a single time scale, $\tau_{\text{early}} \equiv (1/k_{MP}P_0)$, as before. During the late stage, $t \gg \tau_{\text{early}}$, where essentially all reactions are of $P-P$ type, one has simple bimolecular kinetics,

$$p \approx \frac{p_\infty}{t/\tau_{\text{late}}+1}, \quad \tau_{\text{late}} \equiv 1/(k_{PP}P_0 p_\infty), \quad (t \gg \tau_{\text{early}}). \tag{13}$$

IV. APPLICATION TO POLYMER–POLYMER REACTION KINETICS

An interesting application of the analysis of Sec. III is the study of polymer–polymer reaction kinetics. Consider a solution or melt of polymer chains whose degree of polymerization is N, a certain fraction of which carry chemically reactive end groups. Theory[11–13] predicts that the "long time" interpolymeric rate constant, k_{PP}, depends algebraically on N,

$$k_{PP}(N) = k_0 \frac{1}{N^\alpha}, \tag{14}$$

where the particular value of the exponent α depends on the concentration regime and whether or not the solution is entangled. For example, $\alpha=1/2$ and $\alpha=3/2$ are predicted for unentangled[13] and entangled[12] melts, respectively. Neither of these fundamental laws has ever been experimentally tested. We propose here a simple experiment to measure the exponent α, based on the analysis of Sec. III.

The proposed experiment involves creation of a mixture of small radicals (M) and "macroradicals" (P). By macroradicals, we mean polymer chains bearing radical end groups. Such a mixture can readily be created, e.g., by laser flash photolysis of an end-labeled polymer precursor such as the one shown in Scheme II.
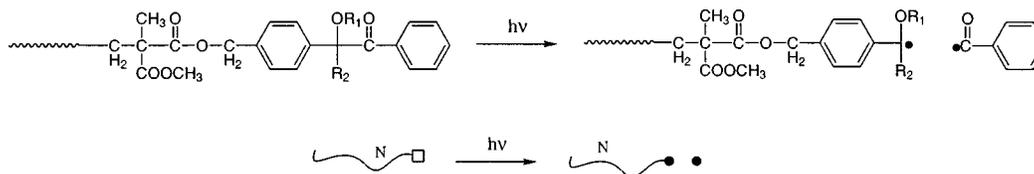
Scheme II.

Note that the ratio of initial densities, r [Eq. (3)], is unity here, guaranteeing that after an initial transient the small radicals will virtually disappear, leaving behind macroradicals only [see Eqs. (11) and (7)]. The time scale for the disappearance of these macroradicals thereafter is τ_{late} of Sec. III [Eq. (13)]. Experimental measurement of $\tau_{\text{late}} \sim 1/k_{PP} \sim N^\alpha$ [from Eqs. (13) and (14)] for different N thus constitutes a direct measurement of the fundamental exponent α.

The above discussion is unfortunately oversimplified. In fact, k_{PP} is time dependent[12,13] for times shorter than the longest relaxation time of the polymers ($t \lesssim \tau_{\text{pol}}$). It is therefore only permissible to use the "long-time" form of k_{PP} of Eq. (14), and hence to apply the analysis of Sec. III, provided $\tau_{\text{pol}} \ll \tau_{\text{early}}$ and $\tau_{\text{pol}} \ll \tau_{\text{late}}$. Now, in concentrated polymer solutions or melts, according to theory,[12,13,33] polymer reaction kinetics is inherently "diffusion-controlled" (DC) and $k_{PP} \approx R^3/\tau_{\text{pol}}$. Here R is the root mean square (rms) polymer coil size. Thus the condition $\tau_{\text{pol}} \ll \tau_{\text{early}}$ leads to

$$P_0 R^3 \ll \epsilon, \tag{15}$$

after using $\tau_{\text{early}} \equiv 1/(k_{MP}P_0)$ [see Eqs. (13) and (9)]. Recall that P_0 is the initial number of macroradicals per unit volume, so the quantity $P_0 R^3$ is the initial volume fraction occupied by the macroradical coils. For example, when $P_0 R^3 = 1$ the coils are just touching one another.

Let us assume then that the initial density is so low that Eq. (15) is satisfied, so the use of the long-time rate constant k_{PP} of Eq. (14) is justified. We now analyze more carefully what happens after the creation of the macroradicals and the small radicals by photolysis which generates macroradical–radical pairs ($r=1$), with the radical groups in very close

proximity to one another. The success of the experiment described above relies on two events: (i) separation (or "escape") of the initial $M-P$ pairs created by the laser pulse, and (ii) the subsequent disappearance of the small radicals, leaving behind the macroradicals. The escape of the macroradical–small radical pairs is discussed in Sec. IV A below. Event (ii) above will occur only if $k_{PP} \ll k_{MP}$ and $k_{PP} \ll k_{MM}$, as discussed in Sec. III. It is clear from Eq. (14) that for large N k_{PP} becomes small compared to k_{MM} (one expects k_{MM} to be the same order of magnitude as the prefactor k_0). But it is not *a priori* obvious that k_{PP} should also be much smaller than k_{MP} [see Eq. (9)]. This is discussed in Sec. IV B below. Finally, we comment on what happens at higher initial densities in Sec. IV C.

A. Escape of the initial macroradical–small radial pairs

Clearly, if the initial macroradical–small radical pairs recombined shortly after their creation by a laser pulse, it would be impossible to isolate the macroradicals. The key quantity which determines whether an initial macroradical–small radical pair escapes is the time integral of the "return probability," $S(t)$. $S(t)$ is the probability that the separation ρ_t between the small radical and the radical group belonging to the macroradical at time t is zero, given that these reactive groups were initially in contact.[11–13,33] Assuming ideal statistics, $S(t)$ is inversely proportional to the volume explored by the rms distance between the reactive groups: $S(t) \approx a^3/\langle \rho_t^2 \rangle^{3/2}$ where a is the monomer size. Now, for sufficiently long times $\langle \rho_t^2 \rangle$ is dominated by the rms displacement, x_t, of the small, fast radical. That is, $\langle \rho_t^2 \rangle \approx x_t^2$ for $t \gg t_a$, where t_a is the relaxation time of both the small radical and that belonging to the macroradical (assumed the same here for simplicity). This is because, for $t \ll \tau_{\text{pol}}$, the rms displacement, x_t^{pol}, of the radical attached to the polymer always grows more slowly in time than the rms displacement of the small radical. (For example, in dilute solutions $x_t^{\text{pol}} \sim t^{1/3}$, while in unentangled melts $x_t^{\text{pol}} \sim t^{1/4}$,[18] compared to the simple Fickian diffusion $x_t \sim t^{1/2}$ for the small radical.) Noting that for the smallest times, $t < t_a$, the radical groups must still be in contact, one has

$$S(t) \approx \begin{cases} (a^3/x_t^3) & (t > t_a) \\ 1 & (t < t_a). \end{cases} \tag{16}$$

Equation (16) above is proved in Appendix B for the case of unentangled melts. It is straightforward to show that Eq. (16) is generally true for other regimes as well: entangled melts, dilute solutions, and semidilute solutions.

Now, a measure of the fraction of the initial pairs that will recombine as $t \to \infty$ is the asymptotic reaction probability

$$\mathscr{R}(t \to \infty) \approx Q \int_0^\infty S(t')dt' \approx Qt_a = \mathscr{O}(1). \tag{17}$$

Here Q is the *local* reaction rate, namely the reaction probability per unit time *given* the reactive groups are in contact. Since $x_t \sim t^{1/2}$, $S(t)$ decays faster than t, from Eq. (16), and the integral is dominated by the smallest times, $t \lesssim t_a$. The
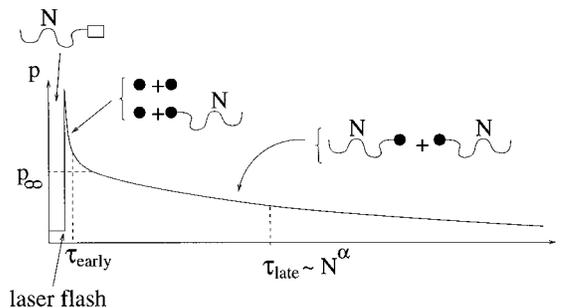

FIG. 6. A solution or melt of polymer chains (degree of polymerization N), a fraction of which carrying photolabile chemical groups is photolyzed by a laser flash at $t=0$, creating a mixture of small radicals and "macroradicals." During an initial transient (time scale τ_{early}) the much more mobile small radicals are consumed through self and cross-coupling reactions, leaving behind a finite fraction p_∞ of the macroradicals. The subsequent much slower kinetics involves essentially only macroradical–macroradical reactions and occurs on a time scale $\tau_{\text{late}} \sim 1/k_{PP} \sim N^\alpha$. Measurement of τ_{late} for different N thus amounts to measuring the fundamental exponent α.

reaction probability per collision, Qt_a, is at most of order unity. The above result tells us that a finite fraction of the initial radical pairs do indeed escape from one another.

B. Subsequent reaction kinetics

We have seen above that a fraction of order unity of the initial macroradical–small radical pairs separate. Following this, radical concentrations start to decay according to the kinetics of Eqs. (2). Now for the subsequent behavior to be the same as that found in Sec. III, we must have $\epsilon \ll 1$ [Eq. (9)]. For large N this is in fact true, because the small radical–macroradical rate constant k_{MP} is dominated by the much higher mobility of the small species. This was shown in Ref. 34: for $N \gg 1$, k_{MP} is independent of N and has a value of the order of the rate constant between two small radicals. That is, k_{MP} is of the same order of magnitude as k_{MM}, which is much larger than k_{PP} [see Eq. (14)]. Thus $\epsilon \ll 1$.

It follows that we can simply take over the analysis of Sec. III, using the expression of Eq. (14) for k_{PP}. The general features of the time development of p kinetic behavior are shown in Fig. 6. After the early transient, during which the small radicals disappear, the late stage kinetics involves only polymer–polymer reactions. Experimentally measuring the concentration of P macroradicals as a function of time, one can thus extract τ_{late} and hence α.

C. Effect of higher initial macroradical densities

We saw that very small densities are required [see Eq. (15)] to justify the use of the long-time rate constant of Eq. (14) and hence the application of the analysis of Sec. III here. In fact we do not have to be so demanding; in order to isolate the macroradicals and measure the exponent α, the condition $P_0 R^3 < 1$ is actually adequate.

Now, strictly speaking, when $P_0 R^3 > \epsilon$, the time dependence of k_{PP} becomes relevant, and hence the analysis of Sec. III is no longer applicable. However, what determines whether or not macroradicals are isolated is the *magnitude* of k_{PP}, which is always small for sufficiently long times. This

is because $k_{PP}(t)$ is a decreasing function of time: e.g., for unentangled melts $k_{PP}(t) \approx k_0(t_a/t)^{1/4}$ for $t_a < t < \tau_{pol}$.[12] Hence for $t \gg t_a$, the conditions $k_{PP} \ll k_{MP}$ and $k_{PP} \ll k_{MM}$ are satisfied even at these higher densities, and one expects all the phenomenology of Sec. III to apply. (Of course a more formal demonstration of this would require more complex analysis to accommodate time-dependent rate constants.)

Note that macroradical densities must, however, be less than the coil overlap threshold ($P_0 R^3 < 1$) in order that the final ''late'' phase of the kinetics can reveal the long-time polymer rate constant k_{PP}; only for such densities is the inequality $\tau_{pol} \ll \tau_{late}$ satisfied. This follows immediately after using the relation $k_{PP} \approx R^3/\tau_{pol}$ in the expression for τ_{late} in Eq. (13). (We assume r is sufficiently bigger than r_c such that p_∞ is of order unity.)

V. DISCUSSION

This work has addressed the transient kinetics of two radical species (M and P) in the particular case where one of these (P) has very low, or zero, self-reactivity. The simplest case where the self-reactivity of the persistent P species is precisely zero is actually quite accurately represented by a number of important radical types (e.g., nitroxides,[10,20] cobalt radicals[29,30]). In this case we have shown that a finite fraction of the P is left behind after the reactions are complete provided the initial concentration ratio, $r \equiv P_0/M_0$, exceeds a certain critical value: $r > r_c^0 \equiv 1 - k_{MM}/k_{MP}$.

It is interesting to compare these results for transient kinetics with those for the analogous steady state situation as studied by Fischer,[9] where the P and M radicals are created continuously at time-independent rates, Q_P and Q_M. In steady state, the quantity most closely corresponding to our parameter r is $\tilde{r} \equiv Q_P/Q_M$. It is simple to show[9] that there is a critical value $\tilde{r}_c = 1$ such that for $\tilde{r} \geq \tilde{r}_c$ the number of P's grows indefinitely and no steady state exists.

The present transient situation is similar, in that there is again a critical value, r_c^0, but the important difference is that this value is now less than unity. Indeed, if it happens that the M self-reactivity is stronger than the cross-coupling reactivity ($k_{MM} > k_{MP}$), then r_c^0 actually becomes negative. In this case a finite fraction of the persistent P species will *always* survive, regardless of the value of the initial concentration ratio, r. This is perhaps our most significant observation.

For most practical situations, the self-reactivity of the P species will be finite, but small: $\epsilon \equiv k_{PP}/k_{MP} \ll 1$. In this case the behavior is very similar to the zero self-reactivity case in that for sufficiently high initial P concentration the nonpersistent M radicals virtually disappear, leaving behind a finite fraction of the initial P radicals. The fundamental difference now is that these isolated P radicals eventually react with one another on a much longer time scale [Eq. (13)]. An interesting and important application of this concept is the study of polymer–polymer reaction kinetics, for which an experiment employing radicals as reactive groups was proposed in Sec. IV.

Experimental data for polymer–polymer reaction kinet-

ics in concentrated solutions and melts is extremely limited and theoretical predictions in these regimes remain largely untested. The most successful method for measuring rate constants k_{PP}, phosphorescence quenching,[15,35] suffers from the limited range of excited state lifetimes: at high concentrations and/or molecular weights the first order decay of excitation competes effectively with the bimolecular quenching events. Experimental data available from phosphorescence quenching experiments on the chain length and concentration dependence of k_{PP} are summarized in Refs. 14 and 11. In the latter, experimental data are also compared with theoretical predictions. For chain length dependence, quantitative experimental data are available for dilute solutions only (to the best of our knowledge), suggesting a power law decay $k_{PP} \sim 1/N^\alpha$ with $0.2 \lesssim \alpha \lesssim 0.3$, with longer chains corresponding to the lower exponents. This is in fairly good agreement with the theoretical prediction[36] for very long chains, $\alpha \approx 0.16$. As for the concentration dependence of k_{PP}, the data of Mita, Horie, and Takeda,[14,37] and of Gebert and Torkelson[15] cover concentrations up to slightly above 30% polymer volume fraction. The observed trend is a decrease of k_{PP} with increasing (inert) polymer concentration at higher concentrations, consistent with theory. However, direct comparison of the data of Mita and Horie[14] with theory is complicated by the fact that the ''reacting'' phosphorescent and quencher end-labeled chains are of different lengths to one another, with inert background chains of yet a third length.

Using radicals in the measurement of k_{PP} offers several advantages. In contrast to phosphorescence quenching, with radicals as reactive groups even in melts, the first order decay of signals can be made negligible compared to the decay due to polymer–polymer reaction events, provided conditions are carefully chosen.[16] An apparent difficulty is that radicals are created in pairs in close proximity to one another; one might expect immediate recombination obviating any long-time measurements. However, in the experiment proposed in Sec. IV, where a mixture of ''macroradicals'' (polymer chains bearing radical end groups) and small molecule radicals are created by a laser flash from polymer chains carrying photosensitive end groups (see Scheme II), it is shown that a finite fraction of the initial small radical–macroradical pairs thus created ''escape,'' even in melts. Following this separation, the small radicals are consumed on a short time scale, leaving behind only the macroradicals, which disappear on a much longer time scale, $\tau_{late} \sim N^\alpha$ (Fig. 6). Hence, monitoring the disappearance of the macroradicals during this long-time scale provides a rather direct measurement of the important exponent α.

Finally, we note that a potentially highly reactive radical may in fact have a very small self-reactivity, and hence qualify as ''persistent,'' for a variety of reasons. This may happen due to classical steric or electrostatic hindrances, as originally suggested by Fischer and Ingold.[9] It may also happen for novel reasons other than simply due to the effect of the local chemical structure on k_{PP}. If one radical species has an extremely low mobility, then we expect to find much of the phenomenology discussed here. Reduced mobility may arise through supramolecular host/guest inter-

actions,[19,38] such as in the case of a mixture of radicals of different sizes confined within a zeolite network. In the latter case, one naively expects that the species whose movement is more severely affected should be more persistent. There are some very recent experimental observations of this type.[39,40] However, we note that one would need to consider the details of these systems more carefully before attempting to apply the simple analysis of Sec. III.

APPENDIX A: PROPERTIES OF THE TRAJECTORIES FOR $\epsilon \neq 0$

In this Appendix we show that, as p decreases, the ratio m/p increases (decreases) for $r < r_c (r > r_c)$. Further, we show that the curvature of the trajectories is always negative when $r < r_c$, and positive when $r > r_c$.

First, the following relationship, valid provided $\omega \neq 0$, is derived from Eq. (10) after use of the variable $v \equiv m/p$,

$$p = \left(\frac{m}{p}\right)^{\epsilon/(1-\epsilon)} \left(\frac{1-r/r_c}{m/p-r/r_c}\right)^{1/\omega+\epsilon/(1-\epsilon)},$$
$$r_c \equiv \omega/(1-\epsilon). \tag{A1}$$

Note that this reduces to Eq. (6) in the limit $\epsilon \to 0$. Note also that one can obtain p^* of Eq. (11) by evaluating the right-hand side of Eq. (A1) at the crossover value of the ratio $m/p \approx \epsilon r$. To leading order in ϵ one obtains $p^* \approx p_\infty$.

Some general features of the trajectories can be obtained either from Eq. (A1), or directly from Eq. (10). Actually it is easier to consider trajectories in the $v-p$ plane. With this transformation of variables, Eq. (10) becomes,

$$\frac{dp}{dv} = \frac{(\epsilon r + v)p}{v(1-\epsilon)(r-vr_c)}. \tag{A2}$$

We are interested in the physically accessible domain $0 \le p \le 1$ and $0 \le v < \infty$. Now trajectories in the $v-p$ plane start from (1,1), and the density p thereafter decreases monotonically to zero. We show below that, as p starts from unity and decreases to zero, (i) for $r > r_c$, v starts from 1 and monotonically decreases to 0, while (ii) for $r < r_c$, v starts from 1 and monotonically increases to ∞.

For $r > r_c$, Eq. (A2) tells us that the slope dp/dv is positive initially when $v = 1$. Therefore, v decreases as p decreases at this point. But from Eq. (A2) this means that dp/dv remains positive, and hence v keeps decreasing as $p \to 0$. But we see that as $p \to 0$ on the left-hand side of Eq. (A1), $m/p = v$ decreases to zero on the right-hand side. On the other hand, for $r < r_c$, Eq. (A2) implies that the initial slope is negative, and v increases as p decreases. This maintains the slope negative, making v increase monotonically as $p \to 0$. From Eq. (A1) we see that now $v \to \infty$ as $p \to 0$.

Translated to the $m-p$ plane, the trajectories for which v lies in the interval (0, 1) are below the critical line $m = p$, as shown in Fig. 5. The curvature for this type of trajectory can

be shown to be always positive by differentiation of Eq. (10) with respect to p, with $r > r_c$. On the other hand, when $1 \le v < \infty$, trajectories in the $m-p$ plane lie above the critical line and the curvature for these is always negative.

APPENDIX B: RETURN PROBABILITY $S(t)$ IN UNENTANGLED MELTS (ROUSE MODEL)

Here we follow Appendix B of Ref. 41. $S(t)$ is the probability density that the group separation ρ_t equals zero, given it was initially zero, i.e.,

$$S(t) = \frac{\langle \delta(\rho_t)\delta(\rho_0)\rangle}{\langle \delta(\rho_0)\rangle}$$
$$= \langle \delta(\rho_t)\rangle|_{\rho_0=0} = \left(\frac{1}{2\pi}\right)^3 \int d^3 \mathbf{k}\langle \exp\{i\mathbf{k}.\rho_t\}\rangle|_{\rho_0=0}$$
$$= \left(\frac{3}{2\pi\langle\rho_t^2\rangle}\right)^{3/2}_{|_{\rho_0=0}}. \tag{B1}$$

We used the fact that ρ_t is Gaussian since Rouse dynamics is linear and forced by Gaussian noise.[18] But $\langle\rho_t^2\rangle|_{\rho_0=0} = \langle x_M^2 + x_P^2\rangle - 2\langle x_M\rangle\langle x_P\rangle = \langle x_M^2 + x_P^2\rangle$. Here x_M and x_P are the rms displacements of the small radical and of the radical attached to the polymer chain end. Now because $x_P \sim t^{1/4}$ (see Ref. 18) grows more slowly than $x_M \sim t^{1/2}$, for $t \gg t_a$ one has $x_M^2 + x_P^2 \approx x_M^2$. Substituted into Eq. (B1), with $x_M \equiv x_t$, this yields Eq. (16) in the main text.

[1] M. J. Perkins, *Radical Chemistry* (Ellis Horwood, New York, 1994).
[2] *Free Radicals*, edited by J. K. Kochi (Wiley New York, 1973).
[3] J. E. Leffler, *An Introduction to Free Radicals* (Wiley, New York, 1993).
[4] G. Wilemski and M. Fixman, J. Chem. Phys. **58**, 4009 (1973).
[5] D. Toussaint and F. Wilczek, J. Chem. Phys. **78**, 2642 (1983).
[6] L. Peliti, J. Phys. A **19**, L365 (1986).
[7] M. von Smoluchowski, Z. Phys. Chem. **92**, 192 (1917).
[8] S. A. Rice, *Diffusion-Limited Reactions* (Elsevier, New York, 1985).
[9] H. Fischer, J. Am. Chem. Soc. **108**, 3925 (1986).
[10] A. L. J. Beckwith, S. Brumby, R. F. Claridge, R. Crocket, and E. Roduner, in *Radical Reaction Rates in Liquids*, edited by H. Fischer (Springer-Verlag, Berlin 1994), Vol. 18. Subvol. a of Landolt-Börnstein Numerical Data and Functional Relationships in Sciences and Technology. New Series. Group II, Atomic and Molecular Physics.
[11] B. Friedman and B. O'Shaughnessy, Int. J. Mod. Phys. B **8**, 2555 (1994).
[12] P. G. de Gennes, J. Chem. Phys. **76**, 3316,3322 (1982).
[13] M. Doi, Chem. Phys. **11**, 115 (1975).
[14] I. Mita and K. Horie, J. Macromol. Sci. Rev. Macromol. Chem. Phys. **C27(1)**, 91 (1987).
[15] M. S. Gebert and J. M. Torkelson, Polymer **31**, 2402 (1990).
[16] N. J. Turro, *Modern Molecular Photochemistry* (University Science Books, Mill Valley, California, 1991).
[17] P. G. de Gennes, *Scaling Concepts in Polymer Physics* (Cornell University Press, Ithaca, 1985).
[18] M. Doi and S. F. Edwards, *The Theory of Polymer Dynamics* (Clarendon, Oxford, 1986).
[19] *Photochemistry in Organized and Constrained Media* edited by V. Ramamurthy (VCH, Weinheim, 1991).
[20] *Spin Labeling II: Theory and Applications* edited by Lawrence J. Berliner (Academic, New York, 1979).
[21] H. Fischer, Macromolecules **30**, 5666 (1997).
[22] R. P. N. Veregin, M. K. Georges, G. K. Hamer, and P. M. Kazmaier, Macromolecules **28**, 4391 (1995).
[23] C. J. Hawker and J. L. Hedrick, Macromolecules **28**, 2993 (1995).
[24] J. C. Scaiano, T. J. Connoly, N. Mohtat, and C. N. Pliva, Can. J. Chem. **75**, 92 (1997).
[25] T. J. Connoly and J. C. Scaiano, Tetrahedron Lett. **38**, 1133 (1997).

[26] E. N. Step, N. J. Turro, N. J. Gande, and P. P. Klemchuk, J. Photochem. Photobiol., A **74**, 203 (1993).

[27] E. N. Step, N. J. Turro, N. J. Gande, and P. P. Klemchuk, Polym. Prepr. (Am. Chem. Soc. Div. Polym. Chem.) **34**, 231 (1993).

[28] D. Ruegge and H. Fischer, Int. J. Chem. Kinet. **21**, 703 (1989).

[29] B. P. Branchaud and G.-X. Yu, Organometallics **12**, 4262 (1993).

[30] B. E. Daikh and R. G. Finke, J. Am. Chem. Soc. **114**, 2938 (1992).

[31] G. Geiger and J. R. Huber, Helv. Chim Acta **64**, 989 (1981).

[32] J. E. Wertz and J. R. Bolton, *Electron Spin Resonance: Elementary Theory and Practical Applications* (McGraw-Hill, New York, 1977).

[33] B. O'Shaughnessy, Phys. Rev. Lett. **71**, 3331 (1993); Macromolecules **27**, 3875 (1994).

[34] B. O'Shaughnessy, Macromol. Theory Simul. **4**, 481 (1995).

[35] J. Guillet, *Polymer Photophysics and Photochemistry* (Cambridge University Press, Cambridge, 1987).

[36] B. Friedman and B. O'Shaughnessy, Europhys. Lett. **23**, 667 (1993); Macromolecules **26**, 5726 (1993).

[37] I. Mita, K. Horie, and M. Takeda, Macromolecules **14**, 1428 (1981).

[38] J.-M. Lehn, *Supramolecular Chemistry: Concepts and Perspectives; A Personal Account* (VCH, Weinheim, 1995).

[39] N. J. Turro, X. Lei, W. Li, A. McDermott, L. Abrams, M. F. Ottaviani, and H. S. Beard, Chem. Commun. **1998**, 695.

[40] N. J. Turro, A. McDermott, X. Lei, W. Li, L. Abrams, M. F. Ottaviani, H. S. Beard, K. N. Houk, B. R. Beno, and P. S. Lee, Chem. Commun. **1998**, 697.

[41] B. Friedman and B. O'Shaughnessy, Macromolecules **26**, 5726 (1993).